Cronfa - Swansea University Open Access Repository

_____

This is an author produced version of a paper published in :

14th British Machine Vision Conference

_____

Cronfa URL for this paper:

http://cronfa.swan.ac.uk/Record/cronfa18017

_____

Conference contribution :

Xie, X. & Mirmehdi, M. (2003). *Geodesic Colour Active Contour Resistent to Weak Edges and Noise.* 14th British Machine Vision Conference, (pp. 399-408). BMVA Press.

http://dx.doi.org/na

_____

Geodesic Colour Active Contour Resistent to Weak Edges and Noise

Xianghua Xie and Majid Mirmehdi
Department of Computer Science,
University of Bristol, Bristol BS8 1UB, England
{xie, majid}@cs.bris.ac.uk

Abstract

The standard geometric or geodesic active contour is a powerful segmentation method, yet it is susceptible to weak edges and image noise. We propose a new region-aided, geometric, colour active contour that integrates gradient flow forces with region constraints. These constraints are composed of image region vector flow forces obtained through the diffusion of the region segmentation map. The extra region force gives the snake a global view of the boundary information within the image which, along with the local gradient flow, helps detect fuzzy boundaries and overcome noisy regions. The partial differential equation (PDE) resulting from this integration of image gradient flow and diffused region flow is implemented using the level set approach.

1 Introduction

The parametric active contour or 'snake', developed by Kass et al. [8], minimises a spline-based deforming curve towards the pull of features such as edges and lines. The energy is composed by terms that control its smoothness and attract it to the object boundary. Region-based parametric snake frameworks have been reported, e.g. [3], however these still suffer from the disadvantages of parametric contours for shape representation.

The geometric model of active contours, simultaneously proposed by Caselles et al. [1] and Malladi et al. [10], avoids the need to reparameterize the curve and is based on the theory of curve evolution in time according to intrinsic geometric measures of the image. It is numerically implemented via level set algorithms [14]. This helps to automatically handle changes in topology and hence, without resorting to dedicated contour tracking, unknown numbers of multiple objects can be detected simultaneously. Furthermore, geometric snakes can have much larger capture areas than parametric snakes. Nevertheless, they still suffer from two significant shortcomings. First, they allow leakage into neighbouring image regions when confronted with weak edges, and second, they may rest at local maximums in noisy images. We handle both these problems in this paper by introducing a diffused region force into the standard geometric snake formulation. The proposed method is referred to as the *Region-aided Geometric Snake* or RAGS to reflect that it integrates gradient flow forces with diffused region forces. The diffused region force is obtained from the region segmentation map vector flow and gives the snake a global view of the object boundaries. The theory is independent of any particular region segmentation technique. We implement the PDE resulting from the proposed method numerically using level set theory [14] which enables topological changes to be dealt with

automatically. In the results section, we illustrate the weak edge improvements and evaluate the tolerance to noise. Moreover, using colour edge gradients (after [13]), the RAGS snake will be shown to naturally extend to object detection in colour images.

There has been a number of works based on the geometric snake and level set framework, e.g. [15, 12, 17]. For example, Siddiqi et al. [15] augmented the performance of the standard geometric snake (that minimises a modified length functional), by combining it with a weighted area functional with an image dependent weighting factor. This resulted in a modification of the constant term of the curve to help it move in the desired direction more efficiently. However, this still did not provide a satisfactory solution to the weak edge leakage problem [15]. Paragios and Deriche [12] presented their Geodesic Active Region model in [12] which initially modeled the image using a Gaussian mixture model to determine the number of regions and their statistics. Then, multiple curves were used to consider each separate homogeneous region and its probabilistically determined boundaries in a bimodal fashion within a geodesic segmentation framework. Their active region model consisted of a region boundary term and a region term which acted as the external pressure force and was implemented via the level set algorithm. In [17], Yezzi et al. developed coupled curve evolution equations and combined them with image statistics for images of a known number of region types (bimodal and trimodal), with every pixel contributing to the statistics of the regions inside and outside an evolving curve.

2   Background

Planar geometric active contours evolve with a velocity vector in the direction normal to the curve using a reaction-diffusion model from mathematical physics [1, 10]. The velocity contains a constant (hyperbolic) motion term that leads to the formation of shocks from which a representation of shapes can be derived, and a (parabolic) curvature term that smooths the front, showing up significant features and shortening the curve. In [2] and [11] the formulation of the geodesic active contour, hereafter also equally referred to as the standard geometric or geodesic snake, was introduced.

For a 2D active contour $C(x,t)$ the Euclidean curve shortening flow is $C_t = \kappa \vec{\mathcal{N}}$, where t denotes time, κ is the Euclidean curvature, and $\vec{\mathcal{N}}$ is the inward unit normal of the contour. Among its many useful properties, this formulation provides the fastest way to reduce the Euclidean curve length in the direction of the gradient of the curve [9]. Given the input image $I : [0,a] \times [0,b] \to \Re^+$ in which the task of extracting an object contour is considered, and the Euclidean length of curve C as $L = \oint |C'(q)| dq$, then the Euclidean length of a curve C in Riemannian space is:

$$L_\Re := \int_0^1 g(|\nabla I(C(q))|)|C'(q)| dq \tag{1}$$

where $g(.)$ represents a decreasing function such that $g(x) \to 0$ as $x \to \infty$, and $g(x) \to 1$ as $x \to 0$. As shown in [2], the steady state is achieved by solving the following equation, showing how each point in the active contour should move in order to decrease the length. The Euler-Lagrange of (1) gives the right-hand side of (2):

$$C_t = g(|\nabla I|)\kappa \vec{\mathcal{N}} - (\nabla g(|\nabla I|) \cdot \vec{\mathcal{N}})\vec{\mathcal{N}} \tag{2}$$

The first term in (2) is the curvature term multiplied by the weighting function $g(.)$ which could be an edge indication function that has larger values in homogeneous regions and

very small values on the edges. Since (2) is slow, Caselles et al. [2] added a constant inflation term $C_t = \vec{\mathcal{N}}$ to speed up the convergence. Integrating it into the geometric snake model lets the curvature flow remain regular:

$$C_t = g(|\nabla I|)(\kappa + c)\vec{\mathcal{N}} - (\nabla g(|\nabla I|) \cdot \vec{\mathcal{N}})\vec{\mathcal{N}} \tag{3}$$

where c is a real constant making the contour shrink or expand to an object boundary at a constant speed in the normal direction. The second term of (2) or (3) acts like a doublet which attracts the snake to the feature of interest since the vectors of ∇g point towards the middle of the boundaries.

Despite their significant advantages, geometric snakes only use local information and suffer from sensitivity to local minima. Hence, they are attracted to noisy pixels and also fail to recognise weaker edges for lack of a better global view of the image. The constant flow term can speed up convergence and push the snake into concavities easily when gradient values at object boundaries are large. But when the object boundary is indistinct or has gaps, it can also force the snake to pass through the boundary. The second term in (3) attracts the contour closer to the object boundary and also pulls back the contour if it leaks through, yet the force may just not be strong enough since it still depends on the gradient values. It can not always prevent weak edge leakage. The left frame in Fig. 1 demonstrates this shortcoming of the standard geometric snake where due to the gradual change of the intensity, the contour leaks through.
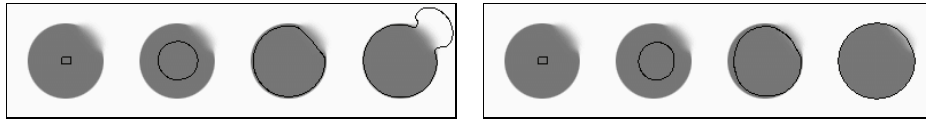

Figure 1: Weak-edge leakage - left frame: geodesic snake steps through; right frame: RAGS snake converges properly using its extra region force.

3 Region-aided Geometric Snake

To make the geometric snake much more tolerant towards weak edges and image noise, we propose a novel approach to integrate the gradient flow force with a diffused region force of the image resulting in our region-aided geometric/geodesic snake, RAGS. The new region-derived force introduces global image features and is aimed at complementing the gradient flow force's local object boundary information. We show that this combination of forces not only improves the performance of the geometric snake towards weak edges, but also makes it more immune to noise. The resulting PDE then evolves an initial contour towards final convergence under the influence of both internal forces and boundary-regional image forces, and can be implemented via level sets.

The gradient flow force is obtained here as in other active contour formulations, e.g. [16, 13, 2, 15, 9]. The new region force can be generated from any image segmentation technique, e.g. [4, 5]. This means that while RAGS is independent of any particular segmentation method, it is dependent on the quality of the regions produced. However, we show a good degree of tolerance to (reasonable) segmentation quality, and that our snake indeed acts as a refinement of the initial region segmentation. To examine this,

we will present results on region maps obtained from both the under-segmentation and over-segmentation options of the software from Comaniciu and Meer [4].

3.1   Region force diffusion

The region force can be generated by a variety of segmentation techniques, greylevel or colour. The segmentation splits the image into several regions. The gradient of this segmentation map gives region constraints in the vicinity of the region boundaries R. While the snake evolves in a homogeneous region, it does so mainly based on the gradient flow force. If the snake tries to step from one region into another, it must concur with the region force since it breaks the region criteria, which probably indicates a leakage. The capture area of the pure region force is quite small. A gradient vector diffusion method was proposed in [16] to extend the gradient map further away from the edges for a larger capture field. We use this same concept to diffuse the region boundary gradient map resulting in region forces with a larger capture area along the region boundaries. Hence, the solution of the generalised region vector flow equation is the equilibrium state of

$$\begin{cases} p(|\nabla R|)\nabla^2 u - q(|\nabla R|)(u - \nabla R_u) = 0 \\ p(|\nabla R|)\nabla^2 v - q(|\nabla R|)(v - \nabla R_v) = 0 \end{cases} \tag{4}$$

where ∇^2 is the Laplacian operator with dimensions u and v, and $p(.)$ and $q(.)$ are weighting functions that control the amount of diffusion. These are selected so that $p(.)$ gets smaller as $q(.)$ becomes larger with the desirable property of little smoothing in the *proximity* of large gradients and the vector field will be nearly equal to the gradient of region map. We use the following functions for diffusing the region gradient vectors:

$$\begin{cases} p(|\nabla R|) = e^{-(|\nabla R/K|)} \\ q(|\nabla R|) = 1 - p(|\nabla R|) \end{cases} \tag{5}$$

with K a constant, acting as a tradeoff between field smoothness and gradient conformity.

3.2   RAGS formulation

The RAGS formulation can be derived by considering the diffused region force as an extra external force of the snake. The original internal and external forces of (3) are given by

$$\begin{cases} F_{int} = g(|\nabla I|)\kappa\vec{\mathcal{N}} \\ F_{ext} = g(|\nabla I|)c\vec{\mathcal{N}} - \nabla g(|\nabla I|) \end{cases} \tag{6}$$

where $g(.)$ is the stopping function as before. Now we add the diffused region force to the external term:

$$F_{ext} = \alpha g(|\nabla I|)\vec{\mathcal{N}} + \beta\tilde{R} - \nabla g(|\nabla I|) \tag{7}$$

where $\tilde{R}$ is the region force vector field obtained in (4), and α is a new constant incorporating and functioning similar to c. Constants α and β act as a tradeoff between gradient and region forces. The snake evolves under all internal and external forces. As only the forces in the normal direction deform the curve, the evolving curve can be represented as

$$C_t = [(F_{int} + F_{ext}) \cdot \vec{\mathcal{N}}]\vec{\mathcal{N}} \tag{8}$$

Finally, the region-aided geometric snake formulation becomes:

$$C_t = [g(|\nabla I|)(\kappa + \alpha) - \nabla g(|\nabla I|) \cdot \vec{\mathcal{N}} + \beta\tilde{R} \cdot \vec{\mathcal{N}}]\vec{\mathcal{N}} \tag{9}$$

3.3 Level set representation

In this section, we outline the level set implementation of RAGS. Level sets describe a moving front and are the basis for the numerical algorithm for curve evolution according to functions of curvature [14]. Let C be a level set of a function of $\phi : [0,a] \times [0,b] \to \Re$, i.e., C is embedded into the zero level set with ϕ an implicit, intrinsic, and parameter free representation of curve C. Given a planar curve that evolves according to $C_t = \mathbb{F}\vec{\mathcal{N}}$ for a given function $\mathbb{F}$, then the embedding function should deform according to $\phi_t = \mathbb{F}|\nabla\phi|$, where $\mathbb{F}$ is computed on the level sets. By embedding the evolution of C in that of ϕ, topological changes of C are handled automatically and accuracy and stability are achieved using the proper numerical algorithm. The internal curvature and external pressure terms of the RAGS formulation in (9) can be easily transferred to a level set representation:

$$
\begin{cases}
C_t = \kappa\vec{\mathcal{N}} & \to & \phi_t = \kappa|\nabla\phi| \\
C_t = g(|\nabla I|)c\vec{\mathcal{N}} & \to & \phi_t = g(|\nabla I|)c|\nabla\phi|
\end{cases}
\tag{10}
$$

The external forces in (9) are static vector fields derived from image data which do not change as the active contour deforms. Static force fields are defined on the spatial positions rather than the active contour itself. Since $\vec{\mathcal{N}}$ is the inward normal, the level set representation of the inward unit normal is given by $\vec{\mathcal{N}} = -\frac{\nabla\phi}{|\nabla\phi|}$. Then we have,

$$
\mathbb{F}\cdot\vec{\mathcal{N}} = -\frac{1}{|\nabla\phi|}(\mathbb{F}\cdot\nabla\phi)
\tag{11}
$$

This leads to the level set representation of RAGS as:

$$
\phi_t = g(|\nabla I|)(\kappa+\alpha)|\nabla\phi| + \nabla g(|\nabla I|)\cdot\nabla\phi - \beta\tilde{R}\cdot\nabla\phi
\tag{12}
$$

where $g(.)$ is the stopping function as before. The expression for the curvature of the zero level set assigned to the interface itself is given by

$$
\kappa = \mathrm{div}\left(\frac{\nabla\phi}{|\nabla\phi|}\right) = \frac{\phi_{xx}\phi_y^2 - 2\phi_y\phi_x\phi_{xy} + \phi_{yy}\phi_x^2}{(\phi_x^2 + \phi_y^2)^{3/2}}
\tag{13}
$$

4 RAGS Snake on Vector-valued Images

The theory of boundary detection by the geometric or geodesic snake can be applied to any general 'edge detector' function [2], with a stopping function g tending to zero when reaching edges. Let f be an edge detector. Then, the decreasing function g can be any decreasing function of f such that $g \to 0$ as $f \to \infty$. When dealing with graylevel images, f and g (as used in this work) are $f = |\nabla(Gauss * I)|$ and $g = (1+f)^{-1}$. For vector-valued images, e.g. a colour image, we apply the approach by di Zenzo [6] to provide a consistent extension of scalar gradients based on a solid theoretical foundation. Such colour edges were also used by [13] and [7] for their geometric and parametric snakes respectively. In a vector-valued image the vector edge is considered as the largest difference between eigenvalues in the tensor metric. Let $\Theta(u_1, u_2) : \Re^2 \to \Re^m$ be a m-band image for $i = 1, 2, ..., m$. For colour images, $m = 3$. The distance between two vector points, $P = (u_1^0, u_2^0)$ and $Q = (u_1^1, u_2^1)$, is given by $\triangle\Theta = \Theta(P) - \Theta(Q)$. When this distance

tends to the infinitesimal, the difference becomes the differential $d\Theta = \sum_{i=1}^{2} \frac{\partial \Theta}{\partial u_i} du_i$ with its squared norm given by

$$d\Theta^2 = \sum_{i=1}^{2} \sum_{j=1}^{2} \frac{\partial \Theta}{\partial u_i} \frac{\partial \Theta}{\partial u_j} du_i du_j \qquad (14)$$

Using standard Riemannian geometry notation, then let $s_{ij} = \frac{\partial \Theta}{\partial u_i} \cdot \frac{\partial \Theta}{\partial u_j}$, such that

$$d\Theta^2 = \sum_{i=1}^{2} \sum_{j=1}^{2} s_{ij} du_i du_j = \begin{bmatrix} du_1 \\ du_2 \end{bmatrix}^T \begin{bmatrix} s_{11} & s_{12} \\ s_{21} & s_{22} \end{bmatrix} \begin{bmatrix} du_1 \\ du_2 \end{bmatrix} \qquad (15)$$

For a unit vector $v = (\cos\theta, \sin\theta)$, then $d\Theta^2(v)$ indicates the rate of change of the image in the direction of v. The extrema of the quadratic form are obtained in the directions of the eigenvectors of the metric tensor s_{ij}, and the corresponding eigenvalues are:

$$\lambda_{\pm} = \frac{s_{11} + s_{22} \pm \sqrt{(s_{11} - s_{22})^2 + 4s_{12}^2}}{2} \qquad (16)$$

with eigenvectors $(\cos\theta_{\pm}, \sin\theta_{\pm})$ where the angles are given by $\theta_+ = \frac{1}{2}\arctan\frac{2s_{12}}{s_{11}-s_{22}}$ and $\theta_- = \theta_+ + \frac{\pi}{2}$. The maximal and minimal rates of change are the eigenvalues (λ_+, λ_-), with corresponding directions of change (θ_+, θ_-). The strength of an edge in a vector-valued case is not given simply by the rate of maximal change λ_+, but by the difference between the extremums. Hence, a good approximation function for the vector edge magnitude should be based on $f = f(\lambda_+, \lambda_-)$. Therefore, we can extend RAGS to the region-aided geometric colour snake by selecting an appropriate edge function f_{col} with the edge stopping function g_{col} defined such that it tends to 0 as $f_{col} \to \infty$ as before:

$$f_{col} = \lambda_+ - \lambda_- \ \text{ and } \ g_{col} = \frac{1}{1 + f_{col}} \qquad (17)$$

Replacing $g_{col}(.)$ for the edge stopping term $g(.)$ in (9), we have the colour RAGS snake:

$$C_t = [g_{col}(|\nabla I|)(\kappa + \alpha) - \nabla g_{col}(|\nabla I|) \cdot \mathscr{N} + \beta \tilde{R} \cdot \mathscr{N}]\mathscr{N}. \qquad (18)$$

Finally, its level set representation is also given by replacing $g_{col}(.)$ for $g(.)$ in (12):

$$\phi_t = g_{col}(|\nabla I|)(\kappa + \alpha)|\nabla\phi| + \nabla g_{col}(|\nabla I|) \cdot \nabla\phi - \beta \tilde{R} \cdot \nabla\phi \qquad (19)$$

5 Analysis and Results

The RAGS (colour) snake propagates under the influence of four forces: (i) the internal curvature flow force, (ii) the pressure force generated by the constant gradient flow, (iii) the gradient of the (colour) edge stopping force, and (iv) the diffused region vector force derived from region constraints. These latter constraints can be generated starting with any region segmentation method. Here, we apply the mean shift algorithm [4] as a general greylevel/colour segmentation technique. This method provides standard pre-set options

for over-segmentation and under-segmentation. We will show results for both of these to illustrate the wide applicability of RAGS.

As shown earlier in Fig. 1, the standard geometric snake steps through the weak edge because the intensity changes so gradually that there is no clear boundary indication in the edge map alone. Weak edges can be handled by RAGS (right frame of Fig. 1) through the extra diffused region force which delivers useful global information about the object boundary and helps prevent the snake from stepping through.

The harmonic shape in Fig. 2 was used to examine RAGS's tolerance to noise. The shape was generated using $r = a + bcos(m\theta + c)$, where a, b, and c remained constant and $m = 6$ was used to produce six 'bumps' [16]. Varying amounts of noise from 10% to 60% was added and the accuracy of fit (i.e. boundary description) after convergence was measured using Maximum Radial Error (MRE), i.e. the maximum distance in the radial direction between the true boundary and the snake. Fig 2 shows the original noisy images in the top row and the region segmentations used for RAGS in the next row (without any post-processing to close gaps etc.). The third and final rows show the converged snake for the standard geometric and RAGS snakes respectively. The initial snake in each case was a square at the edge of the image. A simple subjective examination clearly demonstrates the superior segmentation quality of the proposed snake. At low rates of noise, both snakes could find the boundary accurately enough. However, at increasing rates ($> 20\%$), more

% noise	0	10	20	30	40	50	60
Stand. Geom. Error	2.00	2.23	5.00	10.00	16.16	15.81	28.17
RAGS Error	2.00	2.00	4.03	3.41	5.22	5.38	5.83

Table 1: Maximum Radial Error comparison for the Harmonic shapes in Fig. 2.
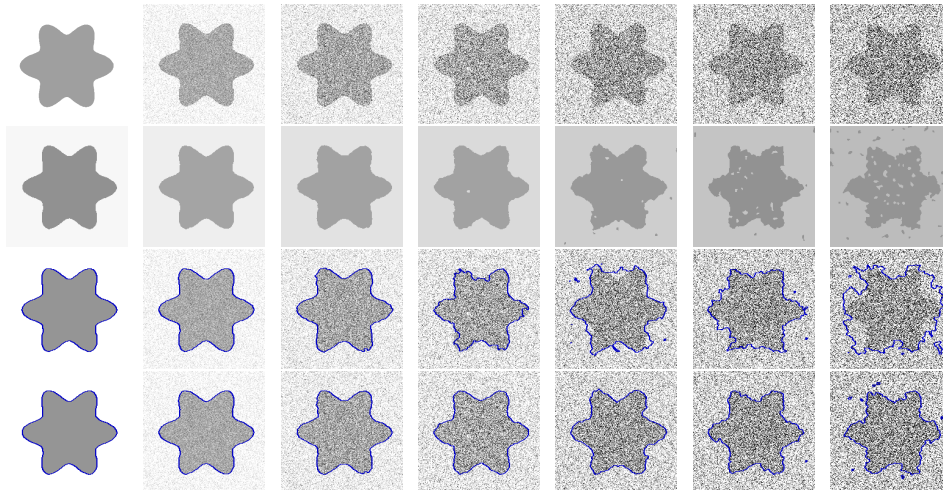

Figure 2: Shape recovery in noisy images - (row 1) original image with various levels of added Gaussian noise [0%,10%,...,60%], (row 2) the region maps later diffused for RAGS; (row 3) standard geometric snake results; (row 4) RAGS results.

and more local maximums appear in the gradient flow force field, preventing the standard geometric snake from converging to the true boundaries. The RAGS snake has a global view of the noisy image and the underlying region force pushes it towards the boundary. The quantitative MRE results are shown in Table 1.

Fig. 3 shows a good example of weak-edge leakage at the right side of the object of interest in a greylevel image. While RAGS does extremely well here, the geometric snake leaks through. Fig. 4 compares the standard geometric snake against the proposed RAGS snake on a colour image of a mouth ulcer. A snake is initialised to detect an inner region which has a small blurred section along its upper boundary. This is again a hard case for the geometric snake because the weak edge is difficult to detect. It not only has similar colour to the inner and outer areas, but also 'dilutes' gradually into the background. Indeed, the standard snake steps through the edge. However, RAGS (last two columns of Fig. 4) reaches its steady state and successfully converges to the inner boundary irrespective of whether the under or over-segmentation of the method in [4] is used to generate the initial region map, as shown.

Fig. 5 demonstrates the improvement over the standard geometric *colour* snake (from [13]). Unlike the latter, RAGS manages to ignore the noisy region in the top right of the image and converges tightly around the object, again due to the stronger diffused region forces at the boundary. In Fig. 6, a close-up view of a retinal disk is shown. The boundary of the optic disk is quite fuzzy and well blended with the background. The region force helps the proposed snake stop at weak edges while the standard geometric snake leaks through. Region segmentation results (under and over-segmentation) with corresponding snakes are also shown. Fig. 7 again shows that RAGS converges on the object very well despite the unsmooth, noisy image regions while the standard snake fails to deal with local maxima of which there are many in the background. Hence, at typical pressure forces it gets stuck in the background. Furthermore, RAGS manages to resolve between the cell outer edge and its nucleus due to the strong nucleus edge information.

6   Conclusions

A novel method, the region-aided geometric snake or RAGS, was proposed. It integrates the gradient flow forces with region constraints, composed by the image region vector flow forces obtained through the diffusion of the region segmentation map. The theory behind RAGS is stand-alone and hence the region force can be generated from any reasonable segmentation technique. We also showed its simple extension to colour gradients. We demonstrated the performance of RAGS, against the standard geometric snake on weak edges and noisy images, as well as on a number of other examples.

We have performed many experiments to verify the resilience of RAGS to weak edges and noise. However, RAGS can suffer from the same shortcomings as the standard geometric snake, or its colour-based relation in [13], in that it will not perform well in highly textured regions where the abundance of edge information will prevent the main object to be reached. It is also dependent on a reasonable segmentation stage, although this was shown to be quite flexible using a popular method with standard built-in options [4].

Further images and results can be found online[1] where we have also extensively compared the RAGS snake against another popular snake, the geometric GGVF snake [16].

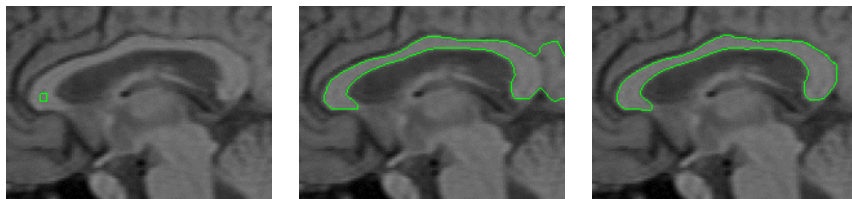
[1] http://www.cs.bris.ac.uk/home/xie/rags.html

Figure 3: Brain MRI - from left: initial, standard geometric, and RAGS snakes.
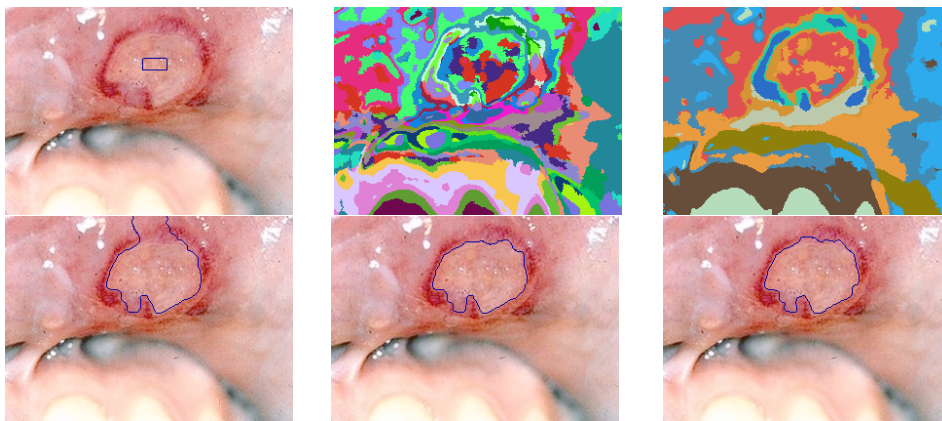

Figure 4: Weak-edge leakage - top row: starting contour, over-segmentation colour regions, and under-segmentation colour regions, bottom row: geodesic snake which steps through and RAGS snake for over and under-segmentation region maps respectively.
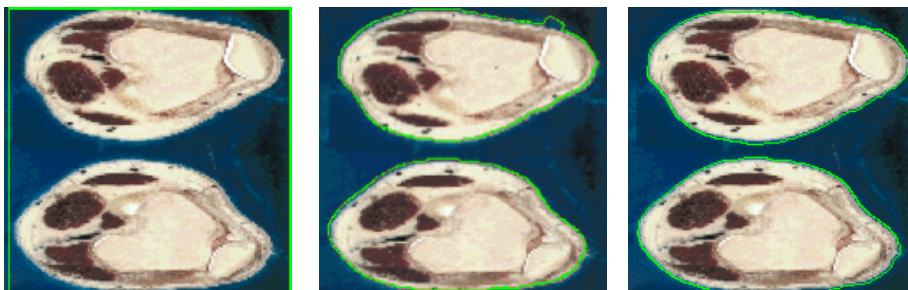

Figure 5: Thigh slice - from left: initial snake, Sapiro's colour snakes [13], RAGS snakes.
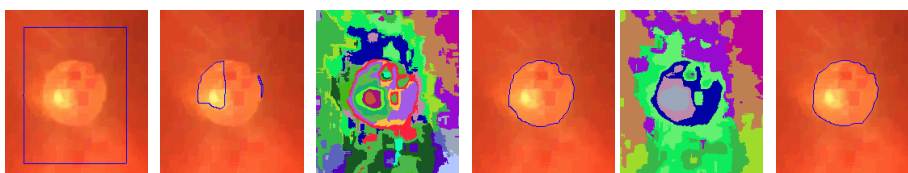

Figure 6: Weak-edge leakage - from left: starting contour, geodesic snake which steps through to the stronger central region, over-segmentation colour regions, and associated RAGS snake, under-segmentation colour regions, and associated RAGS snake.

Figure 7: Bacteria - from left: initial snake, standard geometric snake, RAGS snake which resolves topographically onto the outer boundary and the nucleus.

References

[1] V. Caselles, F. Catte, T. Coll, and F. Dibos. A geometric model for active contours. *Numerische Mathematik*, 66:1–31, 1993.

[2] V. Caselles, R. Kimmel, and G. Sapiro. Geodesic active contour. *IJCV*, 22(1):61–79, 1997.

[3] A. Chakraborty, L. Staib, and J. Duncan. Deformable boundary finding in medical images by integrating gradient and region information. *IEEE-MI*, 15(6):859–870, 1996.

[4] D. Comaniciu and P. Meer. Mean shift: A robust approach toward feature space analysis. *IEEE-PAMI*, 24(5):603–619, 2002.

[5] Y. Deng and B. Manjunath. Unsupervised segmentation of color-texture regions in images and video. *IEEE-PAMI*, 23(8):800–810, 2001.

[6] S. di Zenzo. A note on the gradient of a multi-image. *CVGIP*, 33(1):116–125, 1986.

[7] T. Gevers, S. Ghebreab, and A. Smeulders. Color invariant snakes. In *Proc. 9th BMVC*, pages 659–670, 1998.

[8] M. Kass, A. Witkin, and D. Terzopoulos. Snakes: Active contour models. *IJCV*, 1:321–331, 1988.

[9] S. Kichenassamy, A. Kumar, P. Olver, A. Tannenbaum, and A. Yezzi. Gradient flows and geometric active contour models. In *Proc. 5th ICCV*, pages 810–815, 1995.

[10] R. Malladi, J. Sethian, and B. Vemuri. Evolutionary fronts for topology independent shape modeling and recovery. In *Proc. 3rd ECCV*, pages 3–13, 1994.

[11] R. Malladi, J. Sethian, and B. Vemuri. Shape modeling with front propagation: A level set approach. *IEEE-PAMI*, 17(2):158–175, 1995.

[12] N. Paragios and R. Deriche. Geodesic active regions: A new framework to deal with frame partition problems in computer vision. *Vis. Comm. & Image Rep.*, 13(1-2):249–268, 2002.

[13] G. Sapiro. Color snakes. *CVIU*, 68(2):247–253, 1997.

[14] J. Sethian. *Level Set Methods: Evolving Interfaces in Geometry, Fluid Mechanics, Computer Vision, and Materials Science*. CUP, 1996.

[15] K. Siddiqi, Y. Lauziere, A. Tannenbaum, and S. Zucker. Area and length minimizing flows for shape segmentation. *IEEE-IP*, 7(3):433–443, 1998.

[16] C. Xu and J. Prince. Generalized gradient vector flow external forces for active contours. *Signal Processing*, 71(2):131–139, 1998.

[17] A. Yezzi, A. Tsai, and A. Willsky. A fully global approach to image segmentation via coupled curve evolution equations. *Vis. Comm. & Image Rep.*, 13(1-2):195–216, 2002.